Inorg. Chem. **2002**, *41*, 5891–5896

High-Spin Molecules: Synthesis, X-ray Characterization, and Magnetic Behavior of Two New Cyano-Bridged $Ni^{II}_9Mo^{V}_6$ and $Ni^{II}_9W^{V}_6$ Clusters with a $S = 12$ Ground State

Federica Bonadio,[†] Mathias Gross,[†] Helen Stoeckli-Evans,[‡] and Silvio Decurtins*[,†]

Departement für Chemie und Biochemie, Universität Bern, Freiestrasse 3, CH-3012 Bern, Switzerland, and Institut de Chimie, Université de Neuchâtel, Avenue Bellevaux 51, CH-2007 Neuchâtel, Switzerland

Received February 26, 2002

The preparations, X-ray structures, and magnetic characterizations are presented for two new pentadecanuclear cluster compounds: $[Ni^{II}\{Ni^{II}(MeOH)_3\}_8(\mu\text{-}CN)_{30}\{M^{V}(CN)_3\}_6]\cdot x MeOH\cdot y H_2O$ ($M^{V} = Mo^{V}$ (**1**) with $x = 17$, $y = 1$; $M^{V} = W^{V}$ (**2**) with $x = 15$, $y = 0$). Both compounds crystallize in the monoclinic space group *C2/c*, with cell dimensions of $a = 28.4957(18)$ Å, $b = 19.2583(10)$ Å, $c = 32.4279(17)$ Å, $\beta = 113.155(6)°$, and $Z = 4$ for **1** and $a = 28.5278(16)$ Å, $b = 19.2008(18)$ Å, $c = 32.4072(17)$ Å, $\beta = 113.727(6)°$, and $Z = 4$ for **2**. The structures of **1** and **2** consist of neutral cluster complexes comprising 15 metal ions, 9 Ni^{II} and 6 M^{V}, all linked by μ-cyano ligands. Magnetic susceptibilities and magnetization measurements of compounds **1** and **2** in the crystalline and dissolved state indicate that these clusters have a $S = 12$ ground state, originating from intracluster ferromagnetic exchange interactions between the μ-cyano-bridged metal ions of the type Ni^{II}–NC–M^{V}. Indeed, these data show clearly that the cluster molecules stay intact in solution. Ac magnetic susceptibility measurements reveal that the cluster compounds exhibit magnetic susceptibility relaxation phenomena at low temperatures since, with nonzero dc fields, χ''_M has a nonzero value that is frequency dependent. However, there appears no out-of-phase (χ''_M) signal in zero dc field down to 1.8 K, which excludes the expected signature for a single molecule magnet. This finding is confirmed with the small uniaxial magnetic anisotropy value for D of 0.015 cm^{-1}, deduced from the high-field, high-frequency EPR measurement, which distinctly reveals a positive sign in D. Obviously, the overall magnetic anisotropy of the compounds is too low, and this may be a consequence of a small single ion magnetic anisotropy combined with the highly symmetric arrangement of the metal ions in the cluster molecule.

Introduction

In the field of molecular magnetism,[1] which is an area that has become increasingly important, single-molecule magnets (SMM's)[2] are of considerable interest since they provide a means to systematically study the chemistry and physics of nanomagnets.[3] Unlike normal magnets, the behavior of SMM's arises from the intrinsic properties of individual molecules. The prerequisites are a high spin multiplicity (S) and a strong enough uniaxial magnetic anisotropy of the molecular compounds. Thus, these molecular compounds can be viewed as slowly relaxing magnetic particles which is due to the presence of an energy barrier for the reversal of the direction of its magnetization. Many examples of SMM's are known to date;[2−12] the most

* To whom correspondence should be addressed. E-mail: silvio.decurtins@iac.unibe.ch.
† Universität Bern.
‡ Université de Neuchâtel.

(1) Kahn, O. *Molecular Magnetism*; Wiley-VCH: Weinheim, Germany, 1993.
(2) Aubin, S. M. J.; Wemple, M. W.; Tsai, H.-L.; Christou, G.; Hendrickson; D. N. *J. Am. Chem. Soc.* **1996**, *118*, 7746.
(3) (a) Awschalom, D. D.; Di Vincenzo, D. P.; Smyth, J. F. *Science* **1992**, *258*, 414. (b) Gunther, L. *Phys. World* **1990**, 28. (c) Awschalom, D. D.; Di Vincenzo, D. P. *Phys. Today* **1995**, *48*, 43.
(4) Castro, S. L.; Sun, Z.; Grant, C. M.; Bollinger, J.; Hendrickson, D. N., Christou, G. *J. Am. Chem. Soc.* **1998**, *120*, 2365.
(5) Barra, A. L.; Caneschi, A.; Cornia, A.; Fabrizi de Biani, F.; Gatteschi, D.; Sangregorio, C.; Sessoli, R.; Storace, L. *J. Am. Chem. Soc.* **1999**, *121*, 5302.
(6) Yoo, J.; Yamaguchi, A.; Nakano, M.; Krzystek, J.; Streib, W. E.; Brunel, L.-C.; Ishimoto, H.; Christou, G.; Hendrickson, D. N. *Inorg. Chem.* **2001**, *40*, 4604.
(7) Boyd, P. D. W.; Li, Q.; Vincent, J. B.; Folting, K.; Chang, H. R.; Streib, W. E.; Huffman, J. C.; Christou, G.; Hendrickson, D. N. *J. Am. Chem.. Soc.* **1988**, *110*, 8537.

10.1021/ic025562t CCC: $22.00
Published on Web 10/09/2002

prominent example is the $Mn_{12}Ac$ cluster compound exhibiting a $S = 10$ ground state.[7−12] However, most of the known SMM's represent only stoichiometric variations belonging to a few product families. Therefore, it is a formidable task for the synthetic chemist working in the field of coordination chemistry to search for new molecular compounds showing magnetic effects which may lead to SMM behavior, which finally helps to expand our knowledge of this phenomenon.

On the basis of these considerations and following our strategy of combining paramagnetic molecular building blocks with paramagnetic metal salts to build up polynuclear transition metal compounds, we have been investigating the use of octacyanometalates, $[M^{V}(CN)_8]^{3-}$, as molecular precursors. Along this line, we have already prepared a pentadecanuclear μ-cyano-bridged cluster compound with a $[Mn^{II}_9Mo^{V}_6]$ core.[13] Analogously, Hashimoto et al.[14] have reported a similar $[Mn^{II}_9W^{V}_6]$ stoichiometry. In both cases, the structurally well-defined cluster compounds exhibit very large spin ground states of $S = {}^{51}/_2$ and $S = {}^{39}/_2$, respectively, which is due to the intracluster magnetic exchange interactions which are mediated through the μ-cyano ligands.[15] However, the magnetic anisotropy of these cluster compounds is clearly too low, which may be explained by the small anisotropy of the Mn^{II} ions and the high symmetry of the cluster molecules.[14] Correspondingly, they do not express the typical SMM behavior at temperatures down to 1.8 K.

Therefore, our further study in this area has been extended to the corresponding Ni^{II} systems. Thus, in this work, we report on the synthesis and structural and magnetic characterization of two new $[Ni^{II}_9M^{V}_6]$ compounds, where $M^{V} = Mo^{V}$ and W^{V}. These compounds exhibit the molecular stoichiometry $[Ni^{II}\{Ni^{II}(MeOH)_3\}_8(\mu\text{-}CN)_{30}\{M^{V}(CN)_3\}_6]$, which analogously leads to neutral cluster molecules corresponding in geometry to Ni^{II}-centered polyhedrons spanned by 14 peripheral metal ions. Both compounds were magnetically characterized in the crystalline and dissolved state, and a spin ground state of $S = 12$ was found.

Experimental Section

Synthesis and Crystal Growth. All chemicals and solvents were used as received. All preparations and manipulations were performed under aerobic conditions. $(NBu_4)_3[Mo(CN)_8]$ and $(NBu_4)_3[W(CN)_8]$ were prepared as described elsewhere.[16] *Warning! Cyanides are extremely toxic and should be handled with caution. Perchlorate salts of metal complexes containing organic ligands are potentially explosive*.

$[Ni^{II}\{Ni^{II}(MeOH)_3\}_8(\mu\text{-}CN)_{30}\{M^{V}(CN)_3\}_6]\cdot x MeOH\cdot y H_2O$ ($M^{V} = Mo^{V}$ (1) with $x = 17$, $y = 1$; $M^{V} = W^{V}$ (2) with $x = 15$, $y = 0$). In a 20 mL conical flask was dissolved $(NBu_4)_3[M^{V}(CN)_8]$ (0.094 mmol) in methanol (6 mL). A solution of $[Ni^{II}(H_2O)_6](ClO_4)_2$ (0.141 mmol) in methanol (4 mL) was then added at room temperature under stirring to give a yellow solution. Slow diffusion of diethyl ether into this solution afforded pale yellow crystals where $M^{V} = Mo^{V}$ and yellow crystals for the W^{V} analogue. The crystals were isolated and washed with a mixture of diethyl ether/methanol (2:1). The crystals were stored in this solvent mixture. UV absorption bands: $(NBu_4)_3[Mo^{V}(CN)_8]$, 388.53 nm; **1**, 378.54 nm; $(NBu_4)_3[W^{V}(CN)_8]$, 357.9 nm; **2**, 347.0 nm.

As the compounds decompose when exposed to air, the physical measurements of the crystalline compounds **1** and **2** were performed in the frozen diethyl ether/methanol stock solvent, whereas, for the experiments in solution, the crystalline compounds have been dissolved in methanol (**1a**, **2a**) and measured in the frozen solvent.

X-ray Crystallography. Intensity data were collected at 153 K on a Stoe image plate diffraction system using Mo Kα graphite-monochromated radiation: image plate distance, 70 mm; ϕ oscillation scans, 0−200° (**1**) and 0−182° (**2**); step $\Delta\phi$, 1.0°; 2θ range, 3.27−52.1°; $d_{max}-d_{min}$, 12.45−0.81 Å. The structure was solved by direct methods using the program SHELXS-97.[17] The refinement and all further calculations were carried out using SHELXL-97.[18] The H atoms were included in calculated positions and treated as riding atoms using SHELXL default parameters. The non-H atoms were refined anisotropically, using weighted full-matrix least-squares on F^2. Crystallographic data are summarized in Table 1.

Physical Measurements. Magnetic susceptibility data (dc and ac modes) were collected on a Quantum Design SQUID magne-

Table 1. Crystallographic Data for $[Ni\{Ni(MeOH)_3\}_8(\mu\text{-}CN)_{30}\{Mo(CN)_3\}_6]\cdot 17MeOH\cdot H_2O$ (**1**) and $[Ni\{Ni(MeOH)_3\}_8(\mu\text{-}CN)_{30}\{W(CN)_3\}_6]\cdot 15MeOH$ (**2**)

param	**1**	**2**
formula	$C_{89}H_{166}N_{48}O_{42}Mo_6Ni_9$	$C_{87.50}H_{158}N_{48}O_{39.50}W_6Ni_9$
fw[a]	3684.73	4146.11
cryst syst	monoclinic	monoclinic
space group	*C2/c*	*C2/c*
a, Å	28.4957(18)	28.5278(16)
b, Å	19.2583(10)	19.2008(18)
c, Å	32.4279(17)	32.4072(17)
β, deg	113.155(6)	113.727(6)
V, Å^3	16312.9(16)	16251(2)
Z	4	4
cryst dimens, mm	0.50 × 0.30 × 0.15	0.55 × 0.20 × 0.15
T (K)	153(2)	153(2)
radiation λ, Å[b]	0.710 73	0.710 73
ρ_{calcd}, g cm^{-3}	1.500	1.695
μ, mm^{-1}	1.534	5.318
R [$I > 2\sigma(I)$][c]	0.0377	0.0379
wR2[d] [$I > 2\sigma(I)$]	0.1007	0.0991
goodness of fit[e]	0.995	0.909

[a] Including solvent molecules. [b] Graphite monochromated radiation. [c] $R = \Sigma(||F_o| - |F_c||)/\Sigma|F_o|$. [d] $wR2 = [\Sigma(w(|F_o|^2 - |F_c|^2)^2)/\Sigma(w|F_o|^4)]^{1/2}$. [e] Gof $= [\Sigma w(|F_0|^2 - |F_c|^2)^2]/(n - p)^{1/2}$, where *n* is the number of reflections and *p* is the number of the refined parameters.

(8) Sessoli, R.; Gatteschi, D.; Caneschi, A.; Novak, M. A. *Nature* **1993**, *365*, 141.
(9) Eppley, H. J.; Tsai, De Vries, N.; Folting, K.; Christou, G.; Hendrickson, D. N. *J. Am. Chem. Soc.* **1995**, *117*, 301.
(10) Thomas, L.; Lionti, F.; Ballou, R.; Gattescchi, D.; Sessoli, R.; Barbara, B. *Nature* **1996**, *383*, 145.
(11) Sun, Z.; Ruiz, D.; Rumberger, E.; Incarvito, C. D.; Folting, K.; Rheingold, L.; Christou, G.; Hendrickson, D. N. *Inorg.Chem.* **1998**, *37*, 4758.
(12) An, J.; Chen, Z.-D.; Zhang, X.-X.; Raubenheimer, H. G.; Esterhuysen, C.; Gao, S.; Xu, G.-X. *J. Chem. Soc., Dalton. Trans.* **2001**, 3352.
(13) Larionova, J.; Gross, M.; Pilkington, M.; Andres, H.; Stoeckli-Evans, H.; Güdel. H. U.; Decurtins, S. *Angew. Chem., Int. Ed. Engl.* **2000**, *39*, 1605.
(14) Zhong, Z. J.; Seino, H.; Mizobe, Y.; Hidai, M.; Fujishima, A.; Ohkoshi, S.; Hashimoto, K. *J. Am. Chem. Soc.* **2000**, *122*, 2952.
(15) Chibotaru, L. F.; Mironov, V. S.; Ceulemans, A. *Angew. Chem., Int. Ed.* **2001**, *40*, 4429.
(16) (a) Furman, N. H.; Miller, C. O. *Inorg. Synth.* **1950**, *3*, 160. (b) Basson, S. S.; Bok, L. D. C.; Eiroder, S. R. *Z. Anorg. Allg. Chem.* **1974**, *268*, 287. (c) Basson, S. S.; Bok, L. D. C.; Eiroder, S. R. *Z. Anorg. Allg. Chem.* **1974**, *268*, 287.
(17) Sheldrick, G. M. SHELXS 97, Program for Crystal Structure Determination. *Acta Crystallogr.* **1990**, *A46*, 467.
(18) Sheldrick, G. M. SHELXL 97, Program for the Refinement of Crystal Structures, Universität Göttingen, Göttingen, Germany, 1997.

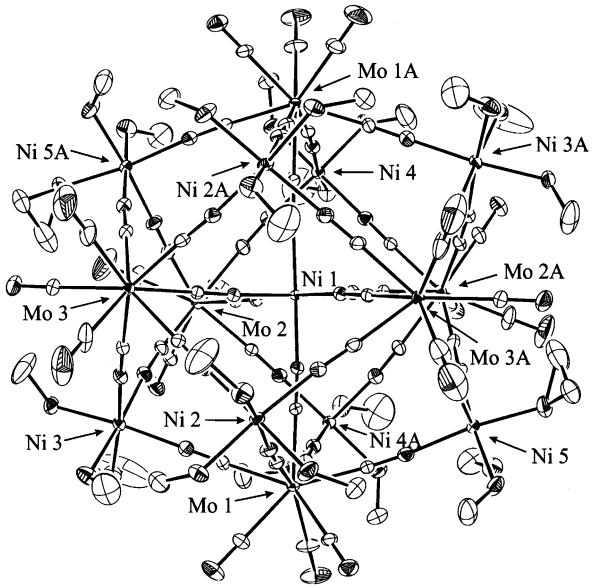

Figure 1. ORTEP representation (ellipsoids at 50% probability) of the molecular structure of the $[Ni\{Ni(MeOH)_3\}_8(\mu\text{-}CN)_{30}\{Mo(CN)_3\}_6]$ cluster (**1**). For clarity only the Ni^{II} and Mo^{V} atoms are labeled and the H atoms are omitted.

tometer (XL5S) equipped with a 50 kG magnet and operating in the temperature range 120−1.8 K. Pascal's constants were used for the diamagnetic corrections for the samples whereas for the diethyl ether/methanol solvent the corrections were determined by using a standard calibrant $HgCo(SCN)_4$ at 120 K. Ac susceptibility data were collected in an ac field of 3.0 G oscillating in the 1−1000 Hz and in an applied dc field of 0.01−10 kG. The sample weights of the crystalline compounds **1** and **2** in the frozen stock solvent were determined by atomic emission spectroscopy (ICP-AES), whereas for the solution measurements in methanol (**1a**, **2a**) the magnetization data for (**1**, **2**) were taken as a reference to give the corresponding weights. EPR measurements were conducted on a polycrystalline sample of **1**, at the high-field, high-frequency EPR facility in Grenoble, France. An excitation frequency of 230 GHz was employed in conjunction with a static field ranging from 0 to 12 T. The experimental setup has been described previously.[19] UV/vis measurements were performed in methanol on $(NBu_4)_3[Mo^{V}(CN)_8]$ and $(NBu_4)_3[W^{V}(CN)_8]$, **1a,b**, with a Lambda 10 Perkin-Elmer UV/vis spectrometer.

Results and Discussion

Description of Structure. The two compounds **1** and **2** are both isostructural to the already reported $[Mn^{II}_9Mo^{V}_6]$ cluster, $[Mn^{II}\{Mn^{II}(MeOH)_3\}_8(\mu\text{-}CN)_{30}\{Mo^{V}(CN)_3\}_6]\cdot 5MeOH\cdot 2H_2O$.[13] A labeled ORTEP plot of a single cluster of **1** is shown in Figure 1, and selected interatomic distances and angles of **1** and **2** are collected in Tables 2−4. Each cluster unit comprises 15 metal ions, 9 Ni^{II} ions and 6 Mo^{V} (W^{V}) ions, all linked by μ-cyano ligands. For simplification, the idealized (O_h symmetry) pentadecanuclear cluster core is sketched in Figure 2. The nine Ni^{II} ions define a body-centered cube, and the six M^{V} ions constitute an octahedron. The central Ni^{II} ion is connected to six Mo^{V} (W^{V}) ions by six μ-cyano ligands. The actual cluster has lower symmetry,

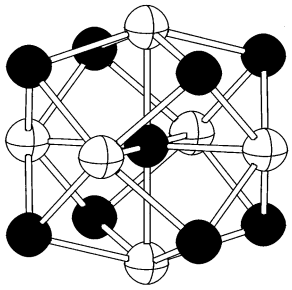

Figure 2. Representation of the $[Ni^{II}_9(\mu\text{-}CN)_{30}M^{V}_6]$ cluster core in an idealized O_h symmetry. The dark spheres represent Ni^{II} ions, and the light spheres, M^{V} ions.

Table 2. Selected Bond Distances (Å) for $[Ni\{Ni(MeOH)_3\}_8(\mu\text{-}CN)_{30}\{Mo(CN)_3\}_6]\cdot 17MeOH\cdot H_2O$ (**1**)

Mo(1)−C(2)	2.145(4)	Ni(1)−Mo(1)	5.315(1)
Mo(2)−C(9)	2.143(4)	Ni(1)−Mo(2)	5.317(1)
Mo(2)−C(17)	2.148(4)	Ni(1)−Mo(3)	5.327(1)
Mo(1)−C(8)	2.150(5)	Ni(2)−Mo(1)	5.347(1)
Mo(3)−C(21)	2.174(4)	Ni(2)−Mo(3A)	5.346(1)
Mo(3)−C(23)	2.149(5)	Ni(2)−Mo(3)	5.333(1)
Mo(3)−C(22)	2.170(4)	Ni(3)−Mo(1)	5.344(1)
Ni(5)−N(8)	2.038(4)	Ni(3)−Mo(2)	5.349(1)
Ni(4)−N(3A)	2.966(4)	Ni(3)−Mo(3)	5.345(1)
Ni(1)−N(2)	2.034(3)	Ni(1)−Ni(2)	6.104(1)
Ni(1)−N(9)	2.039(3)	Ni(1)−Ni(3)	6.263(1)
Ni(1)−N(17)	2.046(3)	Ni(1)−Ni(4)	6.166(1)
Ni(2)−O(1)	2.055(3)	Ni(1)−Ni(5)	6.172(1)
Ni(2)−O(3)	2.091(3)	Ni(2)−Ni(2A)	6.531(1)
C(2)−N(2)	1.139(5)	Ni(4)−Ni(5A)	6.667(1)
C(9)−N(9)	1.135(5)	Ni(5A)−Ni(3)	7.268(1)
C(17)−N(17)	1.136(5)	Mo(1)−Mo(3A)	7.348(1)
C(3)−N(3)	1.131(5)	Mo(3)−Mo(2)	7.443(1)
C(10)−N(10)	1.144(6)	Mo(1)−Mo(2)	7.492(1)
C(15)−N(15)	1.132(7)	Mo(1)−Mo(2A)	7.761(1)
C(12)−N(12)	1.152(6)	Mo(3)−Mo(3A)	7.854(1)

Table 3. Selected Bond Distances (Å) for $[Ni\{Ni(MeOH)_3\}_8(\mu\text{-}CN)_{30}\{W(CN)_3\}_6]\cdot 15MeOH$ (**2**)

W(1)−C(2)	2.149(9)	Ni(1)−W(1)	5.318(1)
W(2)−C(9)	2.164(8)	Ni(1)−W(2)	5.324(1)
W(3)−C(17)	2.165(8)	Ni(1)−W(3)	5.330(1)
W(1)−C(8)	2.144(9)	Ni(2)−W(1)	5.342(1)
W(2)−C(10)	2.184(10)	Ni(2)−W(3A)	5.346(1)
W(2)−C(17)	2.137(9)	Ni(2)−W(3)	5.340(1)
W(3)−C(22)	2.184(8)	Ni(3)−W(1)	5.340(1)
Ni(2)−N(18)	2.034(7)	Ni(3)−W(2)	5.348(1)
Ni(4)−N(3A)	2.059(8)	Ni(3)−W(3)	5.341(1)
Ni(1)−N(2)	2.036(8)	Ni(1)−Ni(2)	6.104(2)
Ni(1)−N(9)	2.047(7)	Ni(1)−Ni(3)	6.257(1)
Ni(1)−N(17)	2.049(7)	Ni(1)−Ni(4)	6.156(2)
Ni(2)−O(1)	2.056(6)	Ni(1)−Ni(5)	6.179(1)
Ni(2)−O(3)	2.088(7)	Ni(2)−Ni(2A)	6.553(2)
C(2)−N(2)	1.138(11)	Ni(4)−Ni(5A)	6.664(2)
C(9)−N(9)	1.111(10)	Ni(5A)−Ni(3)	7.275(2)
C(17)−N(17)	1.120(10)	W(1)−W(3A)	7.345(1)
C(3)−N(3)	1.132(11)	W(3)−W(2)	7.444(1)
C(19)−N(19A)	1.154(11)	W(1)−W(2)	7.493(1)
C(7)−N(7)	1.117(13)	W(1)−W(2A)	7.770(1)
C(4)−N(4)	1.162(11)	W(3)−W(3A)	7.853(1)

C_2, since the compounds crystallize in the monoclinic space group $C2/c$. The crystallographic 2-fold rotation axis runs through the central Ni^{II} ion. For the peripheral metal ions, additional ligands complete their coordination spheres. Each Mo^{V} (W^{V}) ion is linked by five μ-cyano ligands to four peripheral Ni^{II} ions and to the central Ni^{II} ion, and three additional terminal cyano ligands establish the 8-fold coordination, corresponding to the $[M^{V}(CN)_8]^{3-}$ stoichiometry of the molecular building block. Each of the eight peripheral Ni^{II} ions is connected by μ-cyano ligands to three Mo^{V} (W^{V})

(19) (a) Muller, F.; Hopkins, A.; Coron, N.; Grynberg, N.; Brunel, L.; C.; Martinez, G. *Rev. Sci. Instrum.* **1989**, *60*, 3681. (b) Barra, A. L.; Brunel, L. C.; Robert, J. B. *Chem. Phys. Lett.* **1990**, *165*, 107.

Table 4. Selected Angles (deg) for $[Ni\{Ni(MeOH)_3\}_8(\mu\text{-}CN)_{30}\{Mo(CN)_3\}_6]\cdot 17MeOH\cdot H_2O$ (**1**) and $[Ni\{Ni(MeOH)_3\}_8(\mu\text{-}CN)_{30}\{W(CN)_3\}_6]\cdot 15MeOH$ (**2**)

1		**2**	
N(9A)−Ni(1)−N(9)	87.9(2)	N(2A)−Ni(1)−N(17)	87.9(3)
N(17)−Ni(1)−N(17A)	94.2(2)	N(17)−Ni(1)−N(17A)	94.1(4)
N(9A)−Ni(1)−N(17)	176.1(1)	N(17)−Ni(1)−N(9A)	176.2(3)
N(18)−Ni(2)−N(5)	90.9(1)	N(18)−Ni(2)−N(5)	90.7(3)
N(18)−Ni(2)−N(19)	94.8(1)	N(8)−Ni(5)−N(16)	94.6(3)
N(19)−Ni(2)−O(1)	87.1(1)	N(19)−Ni(2)−O(1)	87.4(3)
N(20)−Ni(3)−O(4)	92.8(1)	N(10)−Ni(3)−O(5)	94.6(3)
N(8)−Ni(5)−O(10)	173.0(1)	N(20)−Ni(3)−O(5)	172.9(3)
N(13A)−Ni(4)−O(9)	177.3(1)	N(21)−Ni(5)−O(12)	177.9(3)
C(21A)−N(21)−Ni(5)	173.1(7)	C(21A)−N(21)−Ni(5)	171.8(3)
C(9)−N(9)−Ni(1)	179.2(4)	C(9)−N(9)−Ni(1)	179.5(9)
C(9)−Mo(2)−C(16)	70.5(1)	C(2)−W(1)−C(3)	70.4(3)
C(9)−Mo(2)−C(10)	74.4(2)	C(9)−W(2)−C(10)	74.0(3)
C(18)−Mo(3)−C(19)	75.5(2)	C(19)−W(3)−C(18)	75.6(3)
C(5)−Mo(1)−C(8)	94.6(2)	C(8)−W(1)−C(5)	95.2(5)
C(14)−Mo(2)−C(10)	142.9(2)	C(5)−W(1)−C(10)	142.2(3)
C(11)−Mo(2)−C(10)	146.1(2)	C(11)−W(2)−C(10)	145.1(3)
C(2)−Mo(1)−C(4)	128.7(2)	C(6)−W(1)−C(4)	128.4(4)
C(15)−Mo(2)−C(9)	138.9(2)	C(6)−W(1)−C(2)	140.7(1)
C(24)−Mo(3)−C(18)	69.4(2)	C(15)−W(2)−C(16)	70.4(4)
C(15)−Mo(2)−C(10)	92.7(2)	C(15)−W(2)−C(10)	91.5(5)
C(15)−Mo(2)−C(11)	103.8(2)	C(15)−W(2)−C(11)	105.7(5)
C(15)−Mo(2)−C(13)	147.4(2)	C(6)−W(1)−C(5)	146.4(4)
N(1)−C(1)−Mo(1)	174.8(4)	N(1)−C(1)−W(1)	174.2(8)
N(12)−C(12)−Mo(2)	179.5(5)	N(6)−C(6)−W(1)	179.4(10)

ions, and three additional methanol molecules per Ni^{II} ion increase their coordination number to 6. The $Ni^{II}-N-C-M^{V}$ bridges are fairly linear ($Ni^{II}-N-C = 171.8-179.5°$; $M^{V}-C-N = 174.2-179.5°$). An extended intermolecular H-bonded network connects each cluster unit in the crystal structure to eight nearest-neighboring clusters. Thereby, ligated MeOH molecules act as donors and terminal CN ligands as acceptors. All the nearest-neighbor contacts between metal ions of different clusters are > 7 Å. All terminal cyano and methanol ligands not involved in intercluster H-bonding interactions form hydrogen bonds with solvent molecules.

Dc Magnetic Susceptibility and Magnetization Measurements. Variable-temperature magnetic susceptibility data were collected for the crystalline and dissolved compounds **1** and **1a** (Figure 3) and **2** and **2a** (Figure 4) in an applied magnetic field of 100 G in the temperature range 1.8−120 K. The experimental values of $\chi_M T$ at 120 K are 24.9 (**1, 1a**) and 25.3 (**2, 2a**) emu K mol^{-1}, all distinctly higher than the calculated value of 13.1 emu K mol^{-1} for a cluster comprising nine uncoupled Ni^{II} ($g = 2.2$, $S = 1$) ions and six M^{V} ($g = 1.98$, $S = 1/2$) ions, suggesting the presence of some intracluster ferromagnetic exchange interactions. The $\chi_M T$ values increase with the lowering of temperature reaching a maximum of of 81.5 at 14 K (**1**), 85.2 at 6 K (**1a**), 81.1 at 15 K (**2**), and 87.6 emu K mol^{-1} at 9 K (**2a**). These low-temperature values may be compared with the 86.0 emu K mol^{-1} value expected for an exchange-coupled cluster with a $S = 12$ ground-state spin value. Overall, the cluster molecules in the crystalline and in the dissolved state show very similar magnetic behavior in these $\chi_M T$ vs T plots, and only close to the liquid-helium temperature regime, possible intercluster antiferromagnetic interactions in the crystalline state lead to a divergent behavior of the curves.

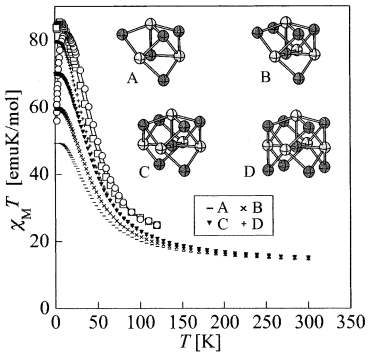

Figure 3. Plot of $\chi_M T$ vs temperature for the polycrystalline compound **1** (○) and for the dissolved compound **1a** (□). The susceptibility was measured under a 100 G magnetic field. The lines A−D represent calculated results (see text) for the corresponding cluster fragments (Ni^{II}, dark spheres; Mo^{V}, light spheres), using $J = 16$ cm^{-1}.

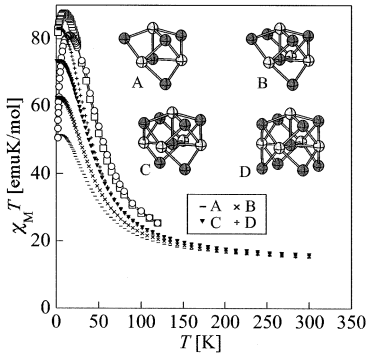

Figure 4. Plot of $\chi_M T$ vs temperature for the polycrystalline compound **2** (○) and for the dissolved compound **2a** (□). The susceptibility was measured under a 100 G magnetic field. The lines A−D, represent calculated results (see text) for the corresponding cluster fragments (Ni^{II}, dark spheres; Mo^{V}, light spheres), using $J = 16$ cm^{-1}.

As a consequence, we conclude that the single cluster molecules stay intact in the dissolved state.

To obtain a rough quantitative estimate of the intracluster exchange interaction parameter J, calculations based on the Hamiltonian $H = -2JS_{Ni}S_M$ were performed. In these calculations we assume only one type of $Ni^{II}-NC-M^{V}$ nearest-neighbor interaction, and consequently, the temperature dependence of $\chi_M T$ is only a function of one single energy parameter, namely J. Despite this simplicity, the calculation of $\chi_M T$ for the whole pentadecanuclear cluster is still beyond our reach, since the total number of electronic cluster states is simply too large; we only reached the limit of 14 metal centers/cluster unit. Therefore, four cluster fragments of increasing size were selected, as illustrated in Figures 3 and 4, and $\chi_M T$ for various J values were calculated using a reported algorithm.[20] From a comparison with the experimental data and considering an extrapolation to the pentadecanuclear cluster unit, a ferromagnetic exchange interaction parameter J on the order of 16 cm^{-1} has been deduced.

Additionally, the field dependences of the magnetization M were measured at 1.8, 5, and 14 K for the compounds **1**, **1a**, **2**, and **2a** under a magnetic field H up to 50 kG and the

(20) Borras-Almenar, J. J.; Clemente-Juan, J. M.; Coronado, E.; Tsukerblat, B. S. *Inorg. Chem.* **1999**, *38*, 6081.

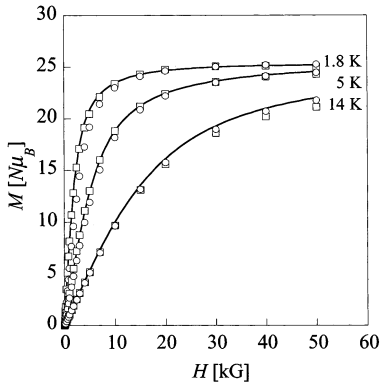

Figure 5. Plot of the field dependences of the magnetization *M* for the polycrystalline compound **1** (○) and for the dissolved compound **1a** (□). The solid lines correspond to the Brillouin functions as described in the text.

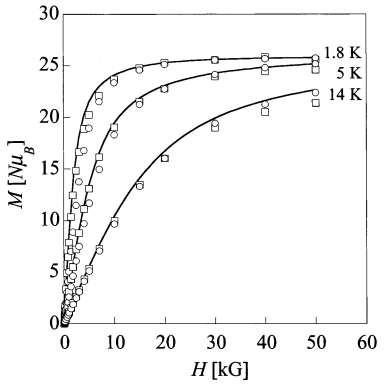

Figure 6. Plot of the field dependences of the magnetization *M* for the polycrystalline compound **2** (○) and for the dissolved compound **2a** (□). The solid lines correspond to the Brillouin functions as described in the text.

curves are shown in Figures 5 and 6 in the form of $M/N\,\mu_B$ vs H, where N and μ_B are Avogadro's number and the electron Bohr magneton, respectively. The data agree with the Brillouin functions for a $S = 12$ state with $g = 2.1$ for $[Ni^{II}_9Mo^{V}_6]$ and $g = 2.15$ for $[Ni^{II}_9W^{V}_6]$. The spin value S corresponds to the value where all the magnetic moments of Ni^{II} and M^{V} atoms are parallel ($S = 9S_{Ni} + 6S_M = 12$).

Ac Magnetic Susceptibility. Because of the occurrence of a high ground-state spin value, the ac susceptibilities for the compounds **1** and **2** were investigated to check for the presence of slow relaxation phenomena. Both compounds show a very similar behavior under these experimental protocols. Some of the data were presented in Figures 7 and 8 for compound **1**. In Figure 7, the out-of-phase ac magnetic susceptibility (χ''_M) measured in dc fields of 0.01, 1, and 10 kG and 3.0 G ac field at a frequency of 30 Hz is plotted against temperature. Clearly, fields of 1 and 10 kG lead to a χ''_M signal moving to high enough temperature to show a peak in the χ''_M vs T plot. Obviously, the sample does exhibit a χ''_M peak at low temperature and the application of an external DC field affects the temperature at which the χ''_M signal is seen. Generally, a peak in χ''_M occurs because, as the temperature is decreased, the thermal energy is reduced to a point where the magnetization of the sample cannot stay in phase with the oscillating ac field. At this point, an out-of-phase component of the ac susceptibility appears. If the

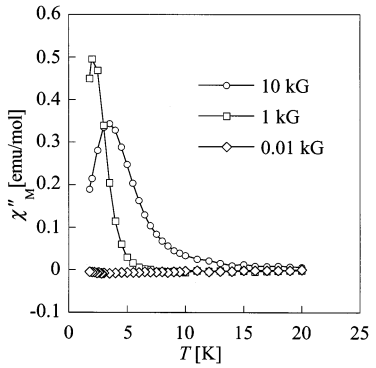

Figure 7. Plots of the out-of-phase ac magnetic susceptibility (χ''_M) vs T for compound **1** in a 3.0 G ac field oscillating at 30 Hz and with applied dc fields of 0.01, 1, and 10 kG.

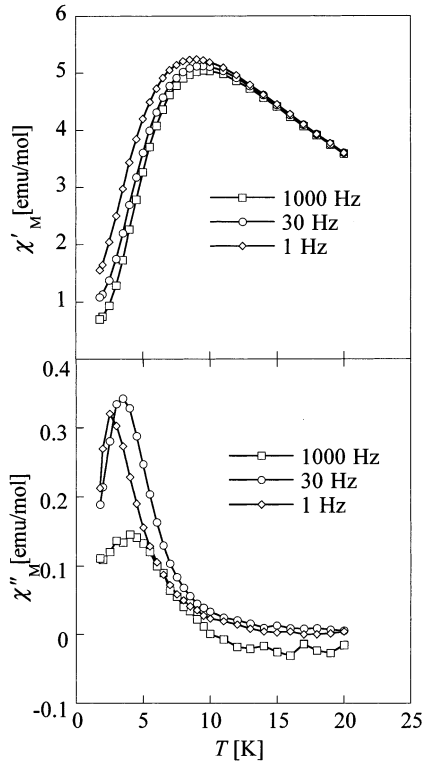

Figure 8. Plot of the in-phase ac magnetic susceptibilities (χ'_M) vs T (top) and out-of-phase ac magnetic susceptibilities (χ''_M) vs T (bottom) for compound **1** in a 3.0 G ac field oscillating at the indicated frequencies and with an applied dc field of 10 kG.

ac frequency is changed, there may be a change in the temperature at which the peak in χ''_M occurs. Thus, the frequency dependence of the χ''_M peak was also studied. In Figure 8, the in-phase (χ'_M) and out-of-phase (χ''_M) ac magnetic susceptibilities measured in a dc field of 10 kG and 3.0 G ac field at frequencies of 1, 30, and 1000 Hz are plotted against temperature. In the 1.8−20 K range, the value of the in-phase ac magnetic susceptibility (χ'_M) exhibits a maximum which is frequency dependent. When (χ'_M) starts to decrease, an (χ''_M) signal appears, for which, with the dc field held constant at 10 kG, an appreciable frequency dependence is seen. As the frequency of the ac field is changed from 1 to 30 to 1000 Hz, the peak in the (χ''_M) signal is shifted from 2.5 to 3.5 to 4 K. In summary, under nonzero dc fields, the compounds exhibit magnetic suscep-

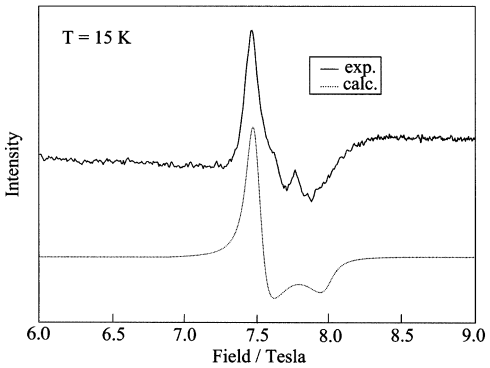

Figure 9. EPR spectrum of **1** recorded at 15 K with an excitation frequency of 230.0000 GHz. The spectral simulation is shown as the broken line and was calculated by numerical diagonalization of the spin-Hamiltonian in eq 1, with $g_{||} = g_{\perp} = 2.15$ and $D = 0.015$ cm^{-1}.

tibility relaxation phenomena at low temperatures since χ''_M has a nonzero value that is frequency dependent. Frequency-dependent χ''_M values are normally seen for superparamagnetic materials.

Finally, the absence of a χ''_M peak with zero dc field indicates that there is no sign of a SMM behavior above 1.8 K.

EPR Measurement. The 15 K, 230 GHz, EPR spectrum between 6 and 9 T of compound **1** is shown as the solid line in Figure 9. The spectrum was interpreted using the spin Hamiltonian for an axial $S = 12$ spin system,[21]

$$\hat{H}_s = g_{||}\mu_B B_Z \hat{S}_Z + g_{\perp}\mu_B(B_X \hat{S}_X + B_Y \hat{S}_Y) + D\left\{\hat{S}_Z^{\,2} - \frac{1}{3}S[S+1)\right\} \quad (1)$$

Further terms, which are allowed from symmetry, were not included, as the information obtainable from the spectrum is limited. Spectral simulations of a powdered sample were calculated by successive numerical diagonalizations of the spin-Hamiltonian, using software written by H. Weihe.[22] The calculated 15 K spectra were found to be very sensitive to the sign and magnitidue of D, and a selection is presented as additional material. The simulated spectrum that best reproduces the experimental data is displayed as the broken line in Figure 9 and was calculated with the spin Hamiltonian parameters, $g_{||} = g_{\perp} = 2.15$ and $D = 0.015$ cm^{-1}. This small and positive anisotropic factor, D, is in accordance with the previous data from the magnetic measurements. Importantly, the positive sign of D for these cluster compounds excludes the occurrence of an energy barrier for reversal of the direction of the magnetic moments which would be needed for a SMM.

(21) Abragram, A.; Bleaney, B. *Electron Paramagnetic Resonance of transition Metal Ions*; Oxford University Press: New York, 1997.
(22) Høgni Weihe, Department of Chemistry, University of Copenhagen.

Concluding Comments

The use of octacyanometalates, $[Mo^V(CN)_8]^{3-}$ and $[W^V(CN)_8]^{3-}$, as molecular precursors and Ni^{II} salts gives rise to neutral, pentadecanuclear cluster compounds held together through 30 μ-cyano bridging ligands. The magnetic exchange interactions within the $[Ni^{II}_9M^V_6]$ cluster core lead to a spin ground state of $S = 12$ for both representatives. The compounds have been characterized in the crystalline and dissolved state, and interestingly, the stay intact in the diluted state. Generally, the use of cluster compounds exhibiting a high ground state spin value and a sharply defined size and solubility will have a benefit in future applications that might require, e.g., thin films. Thus, confirming the retention of structural and therefore magnetic integrity of high-spin cluster compounds on dissolution of the solid compound is therefore important. Ac magnetic susceptibility measurements reveal that these compounds exhibit magnetic susceptibility relaxation phenomena. However, the overall magnetic anisotropy of these specific cluster molecules is too small for expressing the characteristic behavior of single-molecule magnets at the experimental temperature regime down to 1.8 K. This conclusion is also founded on an EPR study which reveals a positive D value for these specific compounds.

Acknowledgment. This work was partially supported by the Swiss National Science Foundation through Project No. 20-61641.00 and the European TMR Research Network entitled "Molecular Magnetism: From Materials toward Devices". The authors thank Dr. Hanspeter Andres, University of Berne, for assistance with the mathematical algorithm, Edith Vogel, University of Berne, for the ICP-AES measurements, and Dr. Philip Tregenna, University of Berne, and Dr. Anne-Laure Barra, CNRS Grenoble, for the EPR data.

Supporting Information Available: Two X-ray crystallographic files, in CIF format. This material is available free of charge via the Internet at http://pubs.acs.org.

IC025562T